

## Computational analysis of the interaction between impregnation, forming and curing in pultrusion

Pierpaolo Carlone<sup>\*1,a</sup>, Ismet Baran<sup>2,b</sup>, Remko Akkerman<sup>2,c</sup>,  
Gaetano S. Palazzo<sup>1,d</sup>

<sup>1</sup> Department of Industrial Engineering, University of Salerno, Via Giovanni Paolo II, 84084 Fisciano, Italy

<sup>2</sup> University of Twente, Faculty of Engineering Technology, NL-7500AE Enschede, The Netherlands

<sup>a</sup>pccarlone@unisa.it, <sup>b</sup>i.baran@utwente.nl, <sup>c</sup>r.akkerman@utwente.nl, <sup>d</sup>gspalazzo@unisa.it

**Keywords:** Pultrusion process, Impregnation, Curing, Stress-strain, Computational analysis.

**Abstract.** Numerical and analytical models dealing with different physics involved in pultrusion are combined in the optic of an integrated analysis of the process. The impregnation stage is simulated by means of a CFD multiphase model, evaluating the pressure and velocity field in the liquid resin. Composite temperature and degree of cure are inferred using 3D thermo-chemical models. Finally, contact conditions, stresses and strains are derived applying computational simulation and analytical models, in order to predict the final pulling force. Different product sizes are considered, simulating suitable processing condition.

### Introduction

Pultrusion is a continuous manufacturing process used to realize constant cross sectional profiles made of polymeric composite materials. Pultruded structures are foreseen to have potential for replacement of conventional materials used in several industries, due to the high effectiveness of the process [1]. For instance, the application of pultruded rods is significantly increasing for reinforcements of concrete elements in the construction industry. What is more, a great deal of interest is currently focused on the potential use of pultruded profiles in offshore wind turbine blades. In this context, a better understanding of the mechanical behavior during processing of pultruded profiles is required. The process follows a multi-step scheme which allows obtaining the final product starting from separated constituents via reinforcement impregnation, work piece forming and composite material consolidation [2]. The fibrous reinforcements are pulled through a catalyzed resin bath and then a heating die. The die inlet is typically characterized by a tapered or conical convergent shape, in order to promote the desired impregnation and compaction of the reinforcement, removing air and excess resin. Then, the heat transferred to the composite material activates the exothermic reaction of the thermosetting resin, resulting also in an internal heat generation and a further temperature increase. The cured and solidified product is continuously advanced via a pulling mechanism and at the end of the process it is cut into the desired length by a cut-off saw. The inherent literature pointed out actual contributes, in terms of process knowledge, achievable by means of process modelling and simulations [3-7]. Several numerical investigations were carried out to simulate pultrusion process, mainly focusing on the temperature and the degree of cure evolutions. Even if the process is conceptually quite simple, the analysis of its dynamics and the definition of optimal processing parameters is a complex task, due to the mutual interactions between involved physical phenomena, mainly related to heat transfer, species conversion and phase changes, die-material contact, and stress-strain development. Early models generally neglected the mutual interaction between involved phenomena, on the base of some simplifying assumptions. Recently, a multi-physics approach, aiming at the evaluation of the different pulling force contributes in pultrusion, was discussed in [8]. In this paper different physics involved in

pultrusion are investigated coupling numerical and analytical models, in the optic of an integrated analysis of the process. The impregnation stage is simulated by means of a CFD multiphase model, evaluating the pressure and velocity field in the liquid resin. Composite temperature and degree of cure are inferred using 3D thermo-chemical models, solved adopting finite element as well as finite volume approaches. Finally, contact conditions, stresses and strains are derived applying computational simulation and analytical models, in order to assess the interaction between the work piece surface and the die. The pultrusion process of a fiber glass/polyester resin cylindrical rod is simulated. Different product sizes are considered, simulating suitable processing condition.

## Process Model

**Impregnation Analysis.** In a conventional pultrusion process, reinforcing fibers are wetted out inside the resin bath before entering the heating die. After the impregnation, wetted fibers typically show an excess of resin with respect to the amount needed in the final product. What is more, a certain amount of air is also contained in the resin. In the tapered zone of the die the processing material is compacted resulting in a pressure increase with respect to the atmospheric value [12,13]. The impregnation model describes the pressure distribution and the resin flow in the first part of the die, including the tapered or rounded zone and a portion of the straight die, by means of the conjunct solution of the well-known mass and momentum equations [8]. In the present investigation a multiphase model was implemented, considering also the presence of entrapped air. A non-homogeneous approach was adopted, solving different sets of equations for each fluid. Under the hypothesis of incompressibility of the fluids and neglecting body forces, the balance equations can be written as:

$$\frac{\partial u}{\partial x} + \frac{\partial v}{\partial y} + \frac{\partial w}{\partial z} = 0, \quad \eta \left( \frac{\partial^2 u}{\partial x^2} + \frac{\partial^2 u}{\partial y^2} + \frac{\partial^2 u}{\partial z^2} \right) - \frac{\partial p}{\partial x} = 0, \quad \eta \left( \frac{\partial^2 v}{\partial x^2} + \frac{\partial^2 v}{\partial y^2} + \frac{\partial^2 v}{\partial z^2} \right) - \frac{\partial p}{\partial y} = 0, \quad \eta \left( \frac{\partial^2 w}{\partial x^2} + \frac{\partial^2 w}{\partial y^2} + \frac{\partial^2 w}{\partial z^2} \right) - \frac{\partial p}{\partial z} = 0, \quad (1)$$

being  $u$ ,  $v$ , and  $w$  the velocity components of the fluid along the  $x$ ,  $y$ , and  $z$  directions and  $p$  the pressure. Resin was modelled as an isothermal-non reactive fluid, considering that the early part of the die is not heated in order to avoid premature resin gelation and temperature and degree of cure (DOC) variations are negligible. Consequently, also resin viscosity was assumed as constant. The reinforcing fibers were treated as a moving porous media, whose porosity and permeability vary according to geometrical considerations, preserving always the final fiber volume. The following modification of the Darcy model has been solved in the porous region:

$$u = U - \frac{K_{xx}}{\eta\Phi} \frac{\partial P}{\partial x}, \quad v = V - \frac{K_{yy}}{\eta\Phi} \frac{\partial P}{\partial y}, \quad w = W - \frac{K_{zz}}{\eta\Phi} \frac{\partial P}{\partial z}, \quad (2)$$

where  $U$ ,  $V$ , and  $W$  represent the velocity components of the porous media along the  $x$ ,  $y$ , and  $z$  directions. Fiber permeability has been defined according to the Gebart model. The impregnation model was solved using the FV scheme available in the commercial software ANSYS-CFX.

**Thermo-chemical Analysis.** Temperature and degree of cure evolution in the die as well as post die region were computed solving the transient energy equation (Eq. 3) in a computational domain including the processing material as well as the heating die. Taking into account that the radius of the reinforcing fibers is quite small, a thermal equilibrium hypothesis applies and the temperature field is established solving a unique nonlinear equation, particularized using lumped material properties [3-8], which can be written as follows:

$$\rho_c C_{p,c} \left( \frac{\partial T}{\partial t} + v_{pul} \frac{\partial T}{\partial z} \right) = k_{x,c} \frac{\partial^2 T}{\partial x^2} + k_{y,c} \frac{\partial^2 T}{\partial y^2} + k_{z,c} \frac{\partial^2 T}{\partial z^2} + V_r q \quad (3)$$

where  $T$  is the temperature,  $t$  is the time,  $\rho_c$  is the density,  $C_{p,c}$  is the specific heat,  $k_{x,c}$ ,  $k_{y,c}$  and  $k_{z,c}$  are the thermal conductivities of the composite material along  $x$ ,  $y$  and  $z$  directions, respectively, and  $V_r$  is the resin volume fraction. Material properties are assumed to be constant throughout the process. The source term  $q$  in Eq. 3 is related to the internal heat generation due to the exothermic resin reaction and expressed as

$$q = \rho_r H_{tr} R_r(\alpha, T), \quad (4)$$

where  $H_{tr}$  is the total heat of reaction for the epoxy resin during the exothermic reaction,  $R_r(\alpha, T)$  is the reaction of cure and  $\rho_r$  is the resin density. The dependence of the reaction rate on the absolute temperature and degree of cure was assumed following a semi-empirical autocatalytic model [11]. Finally, the distributions of the degree of cure and reaction rate were obtained by means of iterative in-house developed routines based on the following discretization:

$$\left( \frac{\partial \alpha}{\partial t} + v_{pul} \frac{\partial \alpha}{\partial z} \right) = R_r(\alpha, T). \quad (6)$$

The above model was solved using a FE approach in the commercial package ABAQUS, as well as a FV approach using the software ANSYS CFX.

**Stress-strain Analysis.** Outcomes provided by the previous models were used to compute thermal and chemical strain contribution in the mechanical (analytical and FEM) models. A plane strain hypothesis is assumed, since the length of the pultruded profiles is much larger than the cross sectional dimensions. The die is assumed to be rigid as compared to the part, hence rigid body surfaces are added at the die-part interface. A mechanical contact formulation is defined at the die-part interface which restricts any expansion of the composite beyond the tool interface; however any separation due to resin shrinkage is allowed. A sliding contact condition between the work piece and the die is considered. A temperature- and cure-dependent resin modulus development is employed using a modified formulation of the CHILE approach [11,12]. The effective mechanical properties of the composite are calculated using the self-consistent field micromechanics (SCFM) relationships, as reported in [7]. More details concerning the derivation of the analytical stress-strain models can be found in [8]. In particular, the analytical model has been modified in order to include also elastic strain terms. In Figure 1, the coupling strategy between the 3D thermo-chemical model and the 2D stress strain models is depicted.

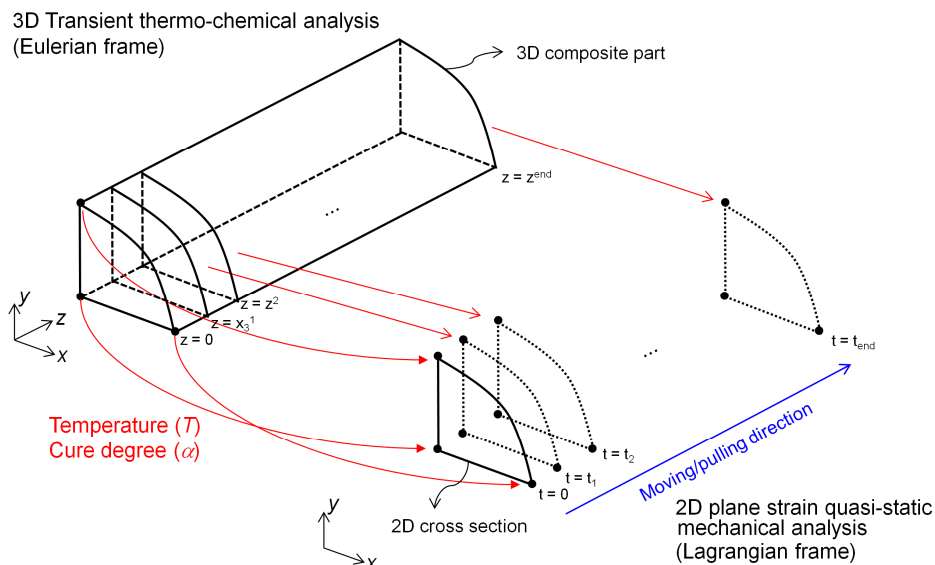


Figure 1: Thermo-chemical and mechanical model coupling.

## Results and Discussions

The simulation of the pultrusion process for a UD fiber glass/polyester composite rod with circular cross section is performed. A scheme of the simulated process is shown in Figure 2. Two different rod radii  $r$  were considered (4.75 mm in case A and 25 mm in case B) to investigate the influence of work piece dimensions on the process features. Following the industrial practice, the pulling speed  $v_{pull}$  was regulated by trial and error in order to achieve a satisfactory degree of cure at the die exit section. In particular  $v_{pull}$  was assumed equal to 10 mm/s (case A) 1.4 mm/s (case B). The exterior surface of the part at the post-die region is exposed to ambient temperature with a convective heat transfer coefficient of 10 W/m-K. The temperature at the die inlet is assumed to be the resin bath temperature (30°C), while the matrix material is assumed to be totally uncured. Only a quarter of the 3D model is considered due to symmetry.

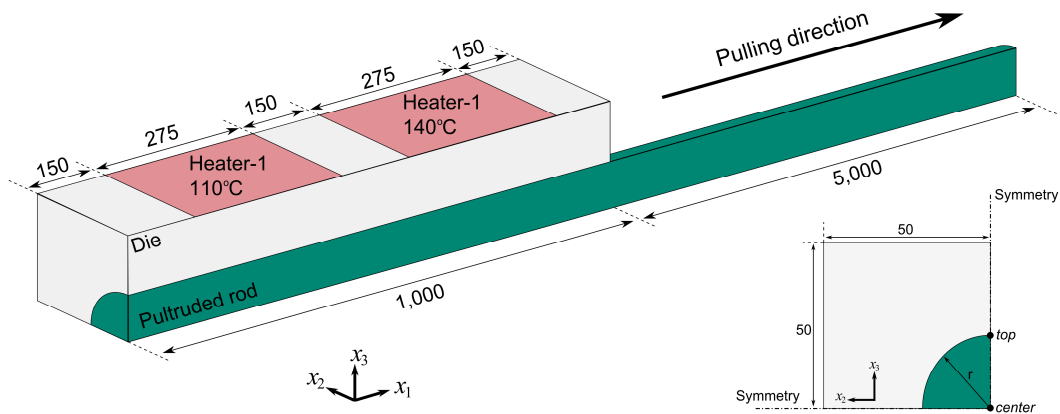


Figure 2: Simulated process

All material properties were assumed according to the characterization discussed in [11,12]. The impregnation model was restricted to the early part of the die, assuming that after this length flow perturbations induced by the convergent section of the inlet vanish. The tapered inlet was modeled following a rounded shape with radius  $R_t$  being equal to 6.35 mm (case A) and 19.05 mm (case B). The preform ratio, defined as the ratio between the cross sectional area of the impregnated material before and after the compaction due to the tapered inlet, is assumed as 1.44.

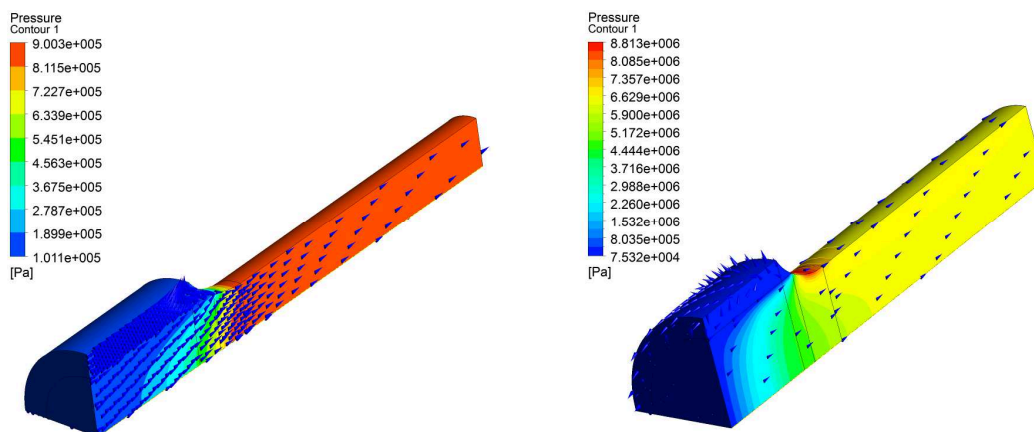


Figure 3: Pressure contours and resin velocity vectors in case A (left) and case B (right)

In Figure 3 some results provided by the impregnation model are reported, showing the pressure distribution in the processing material, as well as a vector plot of the velocity of the resin flow in the tapered region. For all the simulated conditions, an increase in the pressure has been predicted before the intersection point (identified by the contact between the reinforced preform and the die internal surface), imputable to the effect of the resin backflow. Computational simulations pointed out also that the resin velocity converges on the pull speed imposed to the reinforcing fibers at the

very beginning of the straight portion of the die. Comparing the two cases, it is possible to appreciate the influence of the pulling speed on the pressure established into the die, compensating the size effect. The remarkable pulling speed reduction in case B resulted in pressure values lower than in case A.

In Figure 4, some results provided by the thermochemical and stress-strain models are depicted. Negligible variations were found using different numerical scheme (FEM – FVM), so only one profile for each variable is reported in the interest of clarity. Numerical predictions highlighted the concomitant effect played by the work-piece dimensions and pull speed relatively to the temperature and degree of cure evolution. Indeed, the major radius considered in case B delayed the temperature increase and cure reaction activation at the center line of the composite rod. In other words, the heat signal travels more to reach the center of the part as the part thickness increases. Consequently, temperature and the degree of cure profiles at the center shift towards die exit. At the same time, in this case the relatively slower movement of the work-piece allows the heat generated by the resin reaction to dissipate into the processing material. Despite the internal heat generation is proved to be more important for thicker parts [13], the pull speed reduction prevents significant hot spots and reduces the temperature peak. In the post die region a slight increase of the degree of cure is estimated. This is well justified considering the high temperature of the composite at die outlet, which allows the center of the cross section to fully cure.

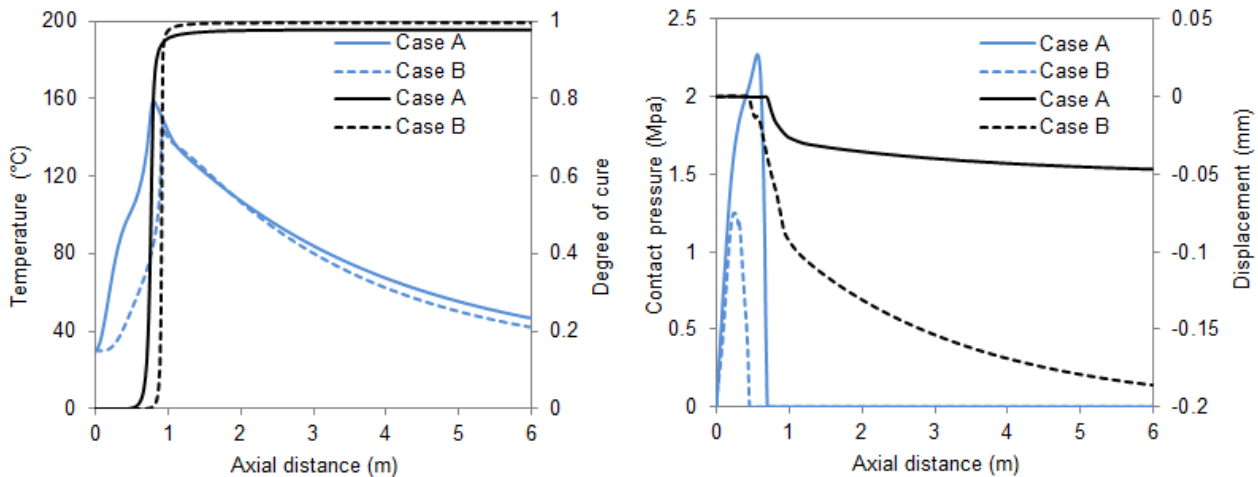


Figure 4. Predicted centerline temperature and degree of cure profiles (*left*) and contact pressure and radius displacement profiles (*right*).

Viscosity profiles directly depend on the temperature and degree of cure evolution. Numerical outcomes evidenced that gelation occurs at a distance of approximately 700 mm (centre) and 500 mm (top) from die entrance in case A and 880 mm (centre) and 200 mm (top) in case B. The relatively major gelation distance observed in case B can be easily related to the size effect. Indeed, the low pull speed promoted an early activation of the cure reaction (and viscosity increase) at the composite external surface, whereas the slower heat conduction delayed the activation of the same reaction at the centre. What is more, taking into account that the gel point separates the liquid zone (where viscous drag acts) from the gel zone (characterized by friction resistance), it follows that a larger the zone interested by viscous force is larger in case A with respect to case B. The viscosity evolution also drives the displacement evolution of the top. The part starts separating from the die surface approximately at 700 mm for case A and 450 mm for case B (see Fig. 4 (*right*)). The maximum in-plane principle stress is found to be approximately 0.5 MPa for case A and 3.5 MPa for case B at the end of the process and it takes place at the centre of the part. This is an expected result because the through-thickness non-uniform curing and thermal history is pronounced more in case B as compared to case A.

The force model described in [8,14] applied to the two cases predicted the following values for the pulling force: approximately 1860 N (being 750 N the viscous force and 1110 N the frictional

force) in case A and 1670 N (being 220 N the viscous force and 1450 N the frictional force). As can be seen, the incidence of each contribution is strongly affected by both pull speed and product size.

### Conclusions

Taking into account what above discussed, the following conclusions can be drawn:

- increasing the rod diameter a reduction of the pull speed is needed to promote a satisfactory cure reaction within the die;
- a resin pressure increase is predicted at the die inlet in both cases, in particular higher pressure is predicted in case A due to the higher pull speed;
- the maximum in-plane principle stress is found to prevail at the center of the part and the stress level is found to be higher in case B then the one in case A.
- a separation at the die-part interface is found to occur at earlier stages for case B as compared to case A which due to different evolution of viscosity in combination with the cure and temperature.

### References

- [1] Y.S. Song, J.R. Youn, T.G. Gutowski, Life cycle energy analysis of fiber-reinforced composites, *Composites: Part A* 40 (2009), 1257–1265.
- [2] T.F. Starr, *Pultrusion for engineers*, Woodhead Publishing Limited, (2000).
- [3] M. Valliappan, J.A. Roux, J.G. Vaughan, E.S. Arafat, Die and post-die temperature and cure in graphite-epoxy composites, *Compos. Part B-Eng* 27 (1996), 1-9.
- [4] Y.R. Chachad, J.A. Roux, J.G. Vaughan, E. Arafat, Three-dimensional characterization of pultruded fiberglass-epoxy composite materials, *J. Reinf. Plast. Comp.* 14 (1995), 495-12.
- [5] I. Baran, J.H. Hattel, C.C. Tutum, Thermo-Chemical Modelling Strategies for the Pultrusion Process, *App. Compos. Mat.* 20 (2013), 1247-1263.
- [6] P. Carlone, G.S. Palazzo, R. Pasquino, Pultrusion manufacturing process development by computational modelling and methods, *Math. Comput. Model.* 44 (2006), 701-709.
- [7] I. Baran, C.C. Tutum, M.W. Nielsen, J.H. Hattel, Process induced residual stresses and distortions in pultrusion, *Compos Part B: Eng* 51 (2013), 148-161.
- [8] P. Carlone, I. Baran, J.H. Hattel, G.S. Palazzo, Computational Approaches for Modeling the Multiphysics in Pultrusion Process, *Advances in Mechanical Engineering 2013* (2013), Article ID 301875, 1-14.
- [9] K.S. Raper, J.A. Roux, T.A. McCarty, J.G. Vaughan, Investigation of the pressure behaviour in a pultrusion die for glass-fibre/epoxy composites, *Compos. Part A* 30 (1999), 1123–1132.
- [10] S.U.K. Gadam, J.A. Roux, T.A. McCarty, J.G. Vaughan, The impact of pultrusion processing parameters on resin pressure rise inside a tapered cylindrical die for glass-fibre/epoxy composites, *Compos. Sci. Tech.* 60 (2000), 945-958.
- [11] I. Baran, R. Akkermann, J.H. Hattel, Material characterization of a polyester resin system for the pultrusion process, *Compos. Part B* 64 (2014), 194-201.
- [12] I. Baran, R. Akkermann, J.H. Hattel, Modelling the pultrusion process of an industrial L-shaped composite profile, *Compos. Struct* 118 (2014), 37-48.
- [13] I. Baran, P. Carlone, J.H. Hattel, G.S. Palazzo R. Akkermann, The effect of product size on the pulling force in pultrusion, *Key, Eng Mat* 611-612 (2014), 1763-1770
- [14] P. Carlone, G.S. Palazzo, Computational Modeling of the Pulling Force in a Conventional Pultrusion Process, *Adv. Mat. Res.* 772 (2013), 399-406.